

# Experimental demonstration of a suspended, diffractively-coupled optical cavity

**M.P. Edgar, B.W. Barr, J. Nelson, M.V. Plissi and K.A. Strain**

Department of Physics and Astronomy, University of Glasgow, Glasgow, G12 8QQ, UK

E-mail: [m.edgar@physics.gla.ac.uk](mailto:m.edgar@physics.gla.ac.uk)

**O. Burmeister, M. Britzger, K. Danzmann, and R. Schnabel**

Max-Planck-Institut für Gravitationsphysik (Albert-Einstein-Institut) and Institut für Gravitationsphysik, Leibniz Universität Hannover, Callinstrasse 38, 30167 Hannover, Germany

**T. Clausnitzer, F. Brückner, E-B. Kley, and A. Tünnermann**

Institut für Angewandte Physik, Friedrich-Schiller-Universität Jena, Max-Wien-Platz 1, 07743 Jena, Germany

**Abstract.** All-reflective optical systems are under consideration for future gravitational wave detector topologies. One approach in proposed designs is to use diffraction gratings as input couplers for Fabry-Perot cavities. We present an experimental demonstration of a fully-suspended, diffractively-coupled cavity and investigate the use of conventional Pound-Drever-Hall length sensing and control techniques to maintain the required operating condition.

A network of first generation laser interferometric gravitational wave detectors (LIGO [1], GEO600 [2], VIRGO [3], and TAMA [4]) is currently operating around the World. All of these instruments are based on enhanced Michelson topologies utilising several techniques to increase the stored laser power and hence detector sensitivity, such as power recycling and optical cavities. Light is coupled in via partially transmissive mirrors and the power in the substrates of some of the optical components such as coupling mirrors or beam splitters reaches or exceeds 1 kW at a wavelength of 1064 nm. Proposed designs for next generation detectors require even higher circulating light levels in order to improve detector sensitivity. Increasing the circulating power is troublesome, since a constant small fraction is absorbed in optical substrates. This causes localised heating which becomes progressively more serious because ever stronger thermal lenses are produced through the change of refractive index with temperature [5]. A potential resolution to this problem is to use all-reflective optical components such as diffraction gratings to split and recombine light fields [6]. A second motivation for the use of gratings in future interferometers arises if cryogenic techniques are required to reduce thermal noise. It is likely that materials that are opaque at 1064 nm, such as silicon, will offer the best performance at cryogenic temperatures and therefore a non-transmissive mechanism must be found.

Although the study of interferometer topologies is essentially straight forward dealing only with the simple relationships among linear light fields, numerical techniques are routinely used to compute the signals obtained at various photodetectors in response to changes in the relative positions of the optics. This is a requirement for the development of length sensing and control schemes required to keep the interferometers at the desired operating point and to read out the signals, including the gravitational wave signal. It is therefore important to understand how to model diffractive couplers and to validate such simulations by experiment.

Several proof-of-principle [7] and bench-top [8] experiments have been carried out to demonstrate the principles of operation for diffractive couplers in optical cavities. In order to examine the applicability to such systems for suspended instruments, one of the arm cavities of the Glasgow 10 m prototype interferometer was commissioned as a diffractively coupled optical cavity (see Figure 1). Each of the optics in this system is suspended as a multi-stage pendulum to provide seismic isolation and allow freedom of motion. The diffraction grating under investigation was manufactured by etching a binary structure into a silica substrate then coating with multiple alternating layers of  $\text{Ta}_2\text{O}_5$  and  $\text{SiO}_2$ , to give an ultra low-loss low-efficiency grating with a period  $d = 1450$  nm [9]. The grating was mounted in 2nd order Littrow configuration, and illuminated at an angle of  $47.2^\circ$  with s-polarised light at 1064 nm wavelength, from a Nd:YAG laser (Model Mephisto 2000NE from Innolight). The configuration chosen provides weak coupling into and out of the cavity ensuring that the resulting system is directly comparable with a conventional Fabry-Perot cavity.

The optical cavities within a gravitational wave detector must be maintained at the correct operating point, usually with the light from the laser resonant (the laser is assumed to be effectively monochromatic, usually this is obtained by suitable feedback control). To this carrier light are added various modulation sidebands, e.g. as prescribed in the Pound-

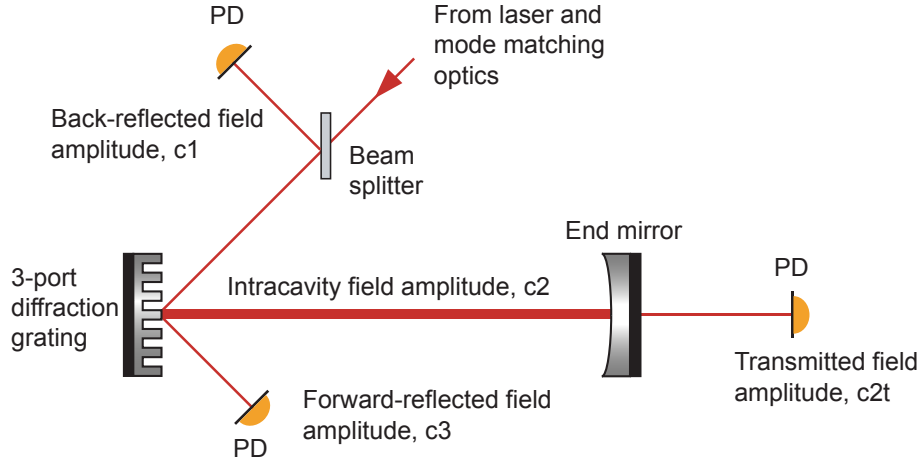


**Figure 1.** Simplified schematic of the three-port second order Littrow mount grating used as the input coupler for a diffractive Fabry-Perot cavity. Tuned photodiodes (PD's) are positioned at all 3 output ports to detect the DC power and RF component for derivation of the control signals.

Drever-Hall (PDH) technique [10] with a particular modulation index. The light leaving the cavity is detected at output ports and information on the interaction between the frequency components can then be extracted by demodulating the detected signals with a local oscillator at the modulation frequency. As seen in Figure 1 our system has 3 detection ports. To enable signal extraction from all three output ports of our diffractive cavity system, two different radio frequency (RF) modulation frequencies were used. As with the normal PDH method, the choice of frequency for the forward and back reflected ports is not critical, provided the sidebands are off-resonance in the cavity when the carrier is resonant. A frequency of 10 MHz was chosen for convenience. On the other hand, to obtain a non-vanishing signal from the transmitted port required the use of sidebands just off-resonance, at 15.24 MHz, close to the free spectral range of the cavity. The transmitted light can subsequently be detected on a tuned photodetector and demodulated to produce a symmetrical length sensing signal.

The operation of a traditional two-port Fabry-Perot cavity is determined by the reflection/transmission efficiencies of the mirrors. However, utilising a three-port diffraction grating as an input coupler to a Fabry-Perot cavity, the optical field interactions become more complex. The scattering matrix of a three-port grating can be represented by:

$$\mathbf{S}_{3p} = \begin{bmatrix} \eta_2 e^{i\phi_2} & \eta_1 e^{i\phi_1} & \eta_0 e^{i\phi_0} \\ \eta_1 e^{i\phi_1} & \rho_0 e^{i\phi_0} & \eta_1 e^{i\phi_1} \\ \eta_0 e^{i\phi_0} & \eta_1 e^{i\phi_1} & \eta_2 e^{i\phi_2} \end{bmatrix}, \quad (1)$$

where  $\eta_{0,1,2}$  and  $\phi_{0,1,2}$  are the amplitude diffraction efficiencies and phase changes on diffraction for zeroth, first and second orders respectively, and  $\rho_0$  is the amplitude reflectivity at normal incidence. If these values are known along with the reflectivity/transmittivity efficiencies of the end mirror then all properties of the cavity can be determined. The input-output relations for a three-port diffraction grating coupled Fabry-Perot cavity have been

Parameter	Value[%]
$\eta_0^2$	99.840
$\eta_1^2$	0.069
$\eta_2^2$	0.016
$\rho_0^2$	99.668

**Table 1.** The parameter values shown were provided by AEI, Hannover where the grating was first tested.

investigated [11] and yield amplitudes for the fields at each port described by:

$$c_1 = \eta_2 e^{i\phi_2} + \eta_1^2 e^{2i(\phi_1 + \phi)} d, \quad (2)$$

$$c_{2t} = i\tau_1 \eta_1 e^{i\phi_1} e^\phi d, \quad (3)$$

$$c_3 = \eta_0 + \eta_1^2 e^{2i(\phi_1 + \phi)} d, \quad (4)$$

where  $\rho_1$  and  $\tau_1$  are the amplitude reflectivity/transmittivity efficiencies of the end mirror and the resonance factor is defined by  $d = [1 - \rho_0 \rho_1 e^{2i\phi}]^{-1}$ .

Based on these field equations a numerical simulation of the diffractive cavity was built using the MATLAB software package, to allow comparison between modelled predictions and experimental results. Using grating parameters provided by the AEI in Hannover and the specifications of the end mirror from the manufacturer, the light field amplitudes and power at each port could be calculated. Direct measurement of the average light power at each output port showed agreement to within 4% of the model.

The diffraction grating properties used in the numerical simulation are presented in Table 1. From these values the loss of the grating can be calculated using the identity  $L_G = 1 - (\rho_0^2 + 2\eta_1^2)$  and it has been determined to be 1940 parts per million (ppm). The calculated finesse of the cavity is then 1143, which is in good agreement with the measured finesse of  $1381 \pm 112$ . The cavity finesse was determined experimentally by measurement of the storage time.

One way to establish whether the sensing signals predicted by the model agree with experiment is to sweep the length of the cavity by at least one round-trip wavelength (one free spectral range in frequency terms). Then the demodulated signal from each port can be compared to the prediction. The slope of this signal at the operating point gives the response for that output port, otherwise known as the effective optical gain. In this experiment, instead of sweeping the cavity length the laser frequency was swept. This has the advantage that it does not risk causing alignment changes of the cavity that could cause higher order cavity modes to become excited thus producing extra features in the result.

The RF signal from each detection port can be demodulated in two orthogonal phases, we call these ‘in-phase’ and ‘quadrature-phase’ respectively. The demodulation phase in the ‘quadrature-phase’ case was adjusted to minimise the signal, while the ‘in-phase’ signal was obtained by adding a precise 90 degree phase shift in the demodulation process. The demodulated signals obtained in the experiment are shown in Figure 2 and are seen to be

in good qualitative agreement with modelled predictions. The discrepancies between the experiment and modelled length sensing signals can be attributed to the finite rate of sweep in the experiment. The model is ‘quasi-static’ and therefore does not predict the slight asymmetry in the patterns seen in the experiment as stored light leaks out after a small delay. There is a practical limit to how slow a sweep can be made due to uncontrolled 1 Hz motion of the pendulums, both longitudinal and causing small misalignments. These effects are almost unavoidable with suspended optics.

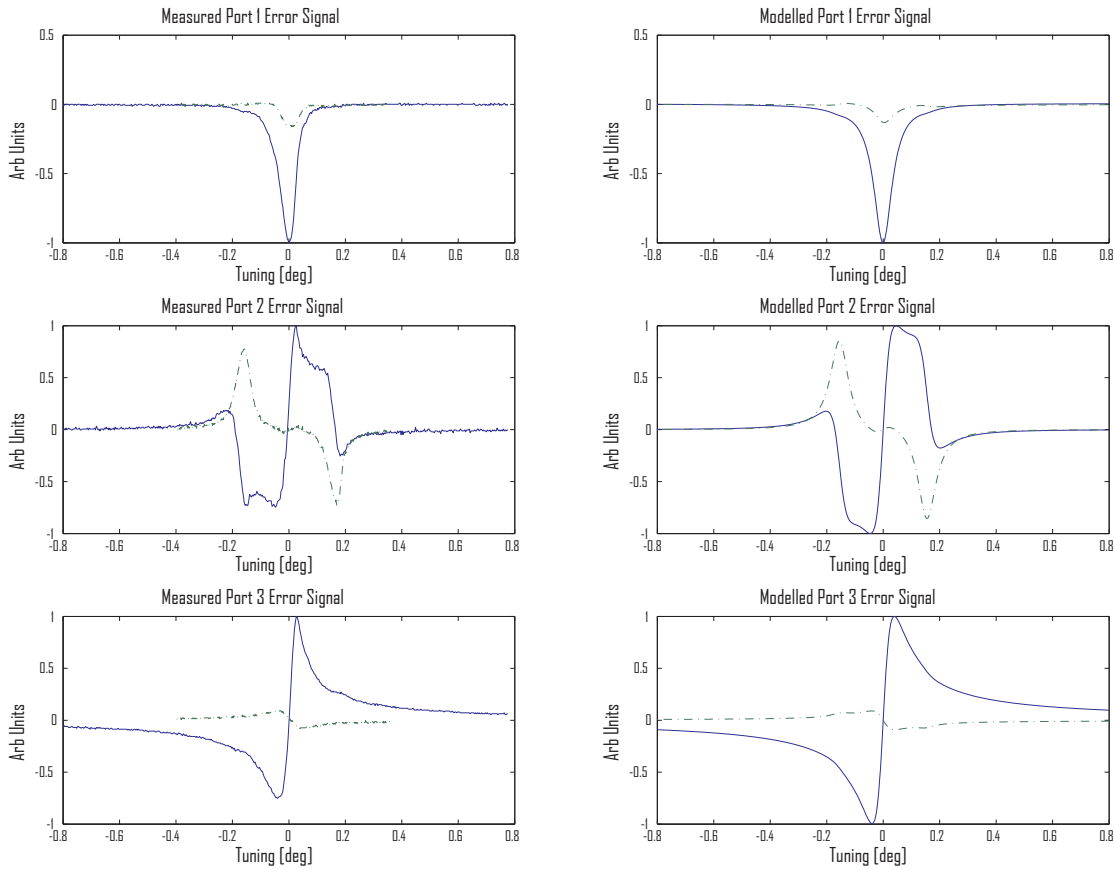


**Figure 2.** Normalised RF power for all three output ports C1 (top), C2 transmitted through ETM (middle), and C3 (bottom). The measured data and modelled predictions of the length sensing signals are presented on the left and right hand side respectively. The solid (blue) trace indicates in-phase measurements, and the dashed (green) trace indicates quadrature-phase. The absolute scaling between modelled ports 1,2 and 3 is 4:1:164 respectively.

To calibrate the demodulated signals detected at all three ports, the relative size of the in-phase slopes were compared to the slope of the signal from the transmitted port. The ratios of the signal responses are presented in Table 2, indicating good quantitative agreement with the model.

Having demonstrated the validity of the model for this experimental configuration, the numerical simulation can be extended to investigate a more general case. In particular,

Parameter	Measured Value[dB]	Modelled Value[dB]
back-reflected/transmitted	-20.910	-20.058
transmitted/transmitted	0	0
forward-reflected/transmitted	49.091	47.179

**Table 2.** The measured and modelled signal response for each port show the correct scaling relative to transmitted port.

previous experimental work with table-top cavities [8] had demonstrated asymmetric behaviour of the reflected carrier power levels. The extent of the asymmetry was seen to be determined by the values of the  $\eta_0$  and  $\eta_2$  diffraction efficiencies. With this in mind, we adapted the numerical simulation to investigate the effects of asymmetry on the demodulated output signals with grating parameters chosen to accentuate the observable effects.

It is clear from the modelled traces (see Figure 3) that the demodulated signals from the forward and back reflected ports do exhibit asymmetry as expected. However, an interesting result of this analysis is that, through careful choice of demodulation phase, we can extract signals from each of these ports which sum together to exactly reconstruct a traditional Pound-Drever-Hall locking signal. Additionally it should be noted that, while the asymmetry is clearly observable for our exaggerated case, the demodulated signals from the forward and back reflected ports will always exhibit some asymmetry - this is limited by the fact that  $\eta_0$  and  $\eta_2$  have a lower bound due to energy conservation [11].

In our experimental configuration the diffractive optic had a second order diffraction efficiency close to the minimum possible, hence the forward reflected signal had a shape that closely resembled the PDH signal. It was possible to lock the cavity using the signal from this port, although not quite at the centre of resonance, therefore the cavity was instead locked to the transmitted error signal (which does exhibit symmetrical behaviour around the centre of resonance). The ability to lock at this known operating point means we can use the diffractively coupled cavity to investigate the dynamic effects associated with suspended optical systems. In particular, when dealing with diffractive couplers phase shifts due to translational motion of the coupler relative to the laser beam are predicted to introduce additional noise when compared to an equivalent traditional cavity configuration [12]. Future experiments on this suspended diffractive system will probe the effect of translational grating motion and associated effects due to cavity misalignment.

In conclusion we have developed a numerical model for length sensing and control signal extraction from a diffractively coupled cavity based on conventional RF sideband modulation and demodulation techniques, and shown the system is well understood through both quantitative and qualitative experimental verification. The experimental results confirm the theoretical foundations supporting a diffractively-coupled Fabry-Perot cavity and successfully demonstrate the use of all-reflective optics in a fully-suspended environment. Based on these findings we have also revealed the effect of grating parameters to signal extraction from a diffractively-coupled system by utilising principles of energy conservation. The framework for signal extraction from a suspended diffractive system is now well understood.

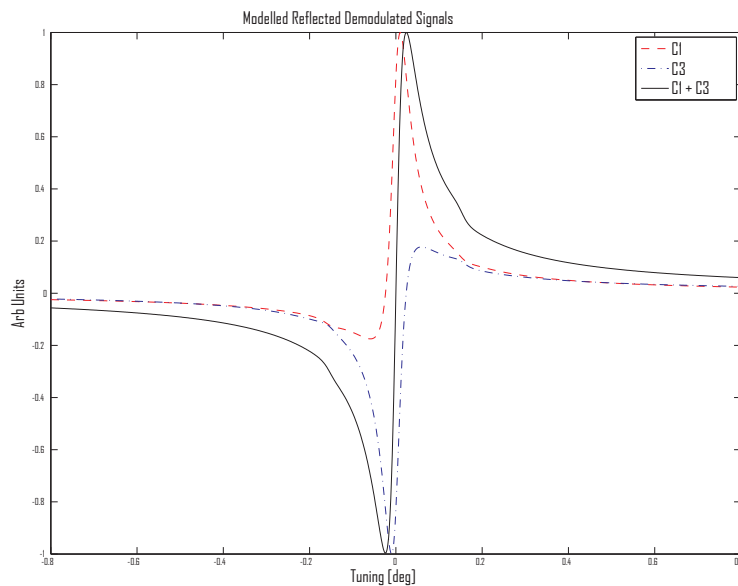


**Figure 3.** Simulated reflected field demodulated signals  $C1$  (red),  $C3$  (blue) and combined  $C1+C3$  (black). The grating parameters chosen here are for an ideal (lossless) grating with  $\rho_0 = 0.99668$ ,  $\eta_1 = 0.0407$ , and  $\eta_0 = \eta_2 = 0.7065$ .

## References

- [1] Sigg D *et al.*, 2002, *Classical and Quantum Gravity* **19** 1429–1435
- [2] Willke B *et al.*, 2002, *Classical and Quantum Gravity* **19** 1377–1387
- [3] Acernese F *et al.*, 2002, *Classical and Quantum Gravity* **19** 1421–1428
- [4] Ando M *et al.*, 2002, *Classical and Quantum Gravity* **19** 1409–1419
- [5] Strain K.A *et al.*, 1994, *Physics Letters A* **194** 124–132
- [6] Bunkowski A *et al.*, 2004, *Optics Letters* **29** 2342–2344
- [7] Sun K.-X *et al.*, 1998, *Optics Letters* **23** 567–569
- [8] Bunkowski A *et al.*, 2006, *Optics Letters* **31** 2384–2386
- [9] Clausnitzer T *et al.*, 2005, *Optics Express* **13** 4370–4378
- [10] Drever R.W.P. *et al.*, 1983, *Applied Physics B* **31** 97–105
- [11] Bunkowski A *et al.*, 2005, *Optics Letters* **30** 1183–1185
- [12] Freise A *et al.*, 2007, *New Journal of Physics* **9** 433